PAPER

Exploring ion migration in Li_2MnSiO_4 for Li-ion batteries through strain effects†

Mingzhen Jia, [ID] [a] Hongyan Wang,*[a] Zhandong Sun,[b] Yuanzheng Chen,[a] Chunsheng Guo [ID] [c] and Liyong Gan [ID] [c]

The orthorhombic crystal Li_2MnSiO_4 is widely studied as a potential high specific energy cathode material for rechargeable batteries. However, low ion diffusion hinders its development. In this paper, first principles calculations were performed to investigate the effect of lattice strain on the ionic diffusion and the defect formation in Li_2MnSiO_4, which are directly related to the rate performance. The computational results show that the Li_2MnSiO_4 material has a two dimensional pathway for effective lithium ion transport, and the Li ion migration barrier is sensitive to the strain applied on the lattice. When strain is applied in *bc* plane, the migration energy increases/decreases with compressive/tensile strain (from −5% to +5%) for both channels. Furthermore, strain applied in *ab* and *ac* planes can also affect Li migration, but the effect is not as obvious as when strain is applied in the *bc* plane. The Li/Mn anti-site defect cannot be produced spontaneously, and the defect formation energy slightly decreases when strain works on the lattice. In fact, an appropriate strain value can improve the rate performance of Li_2MnSiO_4 effectively for applications.

1. Introduction

The high energy and power density of Li-ion rechargeable batteries have been focused on since the development of electric vehicles, portable electronics and large-scale grid storage.[1,2] However, most batteries deliver capacities far below their theoretical values in practical use. One important reason is the low ionic diffusion or electronic conductivity of the electrode materials.[3,4] Research into electrode materials plays a major role in the development of lithium ion batteries. Much attention has been concentrated on the development of electrode technology, in particular for the cathode material, which is the most expensive and capacity limiting component in battery systems.[5]

In search of various cathode materials, Nytén *et al.*[6] first successfully synthesized the Li_2FeSiO_4 material in 2005. The family of Li_2MSiO_4 (M = Mn, Fe, Co, Ni) silicate materials has attracted much attention as potential materials for Li-ion batteries,[7] because these compounds' elements are abundant, low cost and environmentally friendly, and two lithium ions could be extracted per formula unit (f.u.) in theoretical work. Li_2CoSiO_4 exhibits a large irreversible capacity in the cycle process, about 170 mA h g^{-1} capacity (1.1 Li per f.u.) at the first

charge and only 60 mA h g^{-1} irreversible capacity in the first discharge.[8] The Ni-based silicate material has not been synthesized experimentally, and theoretical calculations pointed out prohibitively high voltages when lithium is extracted from Li_2NiSiO_4.[5,9] In 2012, Rangappa *et al.*[10] prepared Li_2FeSiO_4 and Li_2MnSiO_4 by a rapid one pot supercritical fluid synthesis method. It is found that the two cathode materials provide a high reversible capacity (about 340 mA h g^{-1} at 45 ± 5 °C) and two lithium ions could be completely extracted/inserted into the structure. Some research also suggests that the second lithium ion is removed more easily from Li_2MnSiO_4 than from Li_2FeSiO_4, because the high oxidation state Mn^{4+} is more accessible than the unusual Fe^{4+} state.[11] Therefore, Li_2MnSiO_4 is one of the most promising cathode materials for lithium ion batteries.

For the pure Li_2MnSiO_4 material, the intrinsic electronic and ionic conductivity is poor, and the capacity has a serious loss upon cycling. So far, there are many methods to improve the performance of the material, such as carbon coating, chemical doping and particle nanosizing. Research suggests that carbon–Li_2MnSiO_4 exhibited a stable discharge behavior and improved electrochemical performance.[12,13] Al, Ga, Fe, Cr, V, *etc.* have been doped to the Li_2MnSiO_4 material,[14–17] and these dopants play an active role in improving the electrochemical properties in some cases. It should be noted that many problems still remain. Recently, some researchers reported that changing the lattice strain could be considered as a useful method to improve the kinetic properties of various cathode materials, as the activation barrier energy is sensitive to the lattice strain. The layered $LiCoO_2$ has a one-dimensional pathway for Li

aSchool of Physical Science and Technology, Southwest Jiaotong University, Key Laboratory of Advanced Technology of Materials, Ministry of Education, Chengdu 610031, China. E-mail: hongyanw@home.swjtu.edu.cn

bDepartment of Physics, University of Debrecen, Debrecen 4026, Hungary

cSuperconductivity and New Energy R&D Center, Southwest Jiaotong University, Mail Stop 165#, Chengdu 610031, China

migration, and first principles calculations show that activation barrier decreases/increases depend on tensile/compressive stress along the c-axis direction between -5% and $+5\%$.[18] For the olivine compounds $LiFePO_4$ and $NaFePO_4$, Tealdi et al.[19] suggested that the strain of the lattice has a remarkable effect on the material, with a major increase of the Li^+ and Na^+ conductivity and a decrease of the blocking defect. Moreover, changing the lattice strain is regarded as an effective method to modulate the properties of materials, such as optics,[20] super-conductivity[21] and conductivity.[22] With the development of technology, some experiments have shown an improvement in the performance of oxide materials for solid oxide fuel cells (SOFCs) by tuning the lattice strain. The lattice strain plays a positive role in ionic migration, oxygen vacancy formation, and oxygen molecule adsorption.[23] For example, the ionic conductivity has been greatly improved, increasing by about five to eight orders of magnitude.[24,25] Thus, researching the lattice strain in the Li_2MnSiO_4 material is necessary.

Controlling the ion dynamics of the electrode material is critical for the Li ion battery. In this paper, we present a density functional theory investigation of a silicate type of Li_2MnSiO_4 material. The influence of the crystal structure under biaxial strain on the ab, ac and bc planes is considered in detail. Then the strain effects on the Li ion migration and defect formation are discussed. So far, there have been no experiments about improving the properties of Li_2MnSiO_4 by controlling the strain. We hope our results could play a guiding role for further practical applications in the future.

2.   Computational details

First principles calculations were performed using the Vienna Ab Initio Simulation Package (VASP) code,[26,27] and core ion and valence electron interactions based on the projector augmented wave (PAW) potentials.[28] The Perdew–Burke–Ernzerhof generalized gradient approximation (PBE-GGA) was used for the exchange–correlation energy.[29] In order to accurately simulate the strong interaction character of the d electrons for the transition-metal ions, the Hubbard-type correction is included.[30]

The lattice parameters, cell volumes and the atomic positions are fully optimized and relaxed until the energy is less than 1.0×10^{-5} eV and the force on each atom is less than 0.02 eV Å^{-1}. We used the conjugate gradient minimization method for geometry optimization. A Monkhorst–Pack grid with $2 \times 2 \times 2$ (for a $2 \times 2 \times 2$ supercell) meshes was employed in the irreducible Brillouin zone.[31] A kinetic energy cutoff of 500 eV was used for the plane-wave. Following previous reports, the effective U_{eff} ($U–J$) is fixed at 5 eV for the Mn-3d state.[32,33] According to the above calculation method, biaxial lattice strain is applied in the ab, ac and bc planes. For the strained systems, in the range of -5% to $+5\%$, the strain value is compared with the relaxed lattice parameters and is applied simultaneously in two crystal axes. The lattice strain, ε, is expressed by the following equation:

$$\varepsilon = \frac{a_s - a_0}{a_0} \qquad (1)$$

where a_s and a_0 are the strained and unstrained lattice parameters, respectively.[34,35] When $\varepsilon > 0$, tensile strain is formed in the structure; otherwise, compressive strain ($\varepsilon < 0$) is formed. Energy minimization of the strain applied structures is based on a series of the third axis parameter and then relaxation of all atomic coordinates, so as to find the one associated with the minimum in the total energy of the structure. A similar approach has been successfully applied to study ion conduction and oxygen transport for SOFC materials.[36,37]

The minimum energy pathways and activation barriers of Li ion migration were calculated using the climbing image nudged elastic band (CI-NEB) method,[38,39] in which a number of images are optimized between the starting point and the end point along the reaction path. The CI-NEB method is a modification of the NEB method. The image is made to climb up along the elastic band to converge rigorously on the highest saddle point.

3.   Results and discussion

3.1   Strain effects on the crystal structure

The structure of Li_2MnSiO_4 was first reported by Dominko et al.[40] in 2006, and it is analogous to that of the Li_2FeSiO_4 (ref. 41) crystal, with the space group $pmn21$ accompanied by a slightly distorted orthorhombic lattice. The lattice parameters are $a = 6.3109(9)$ Å, $b = 5.3800(9)$ Å, $c = 4.9662(8)$ Å, and $\alpha = \beta = \gamma = 90°$. The Li_2MnSiO_4 compound has a rich polymorphism with a series of $[MnO_4]$, $[SiO_4]$ and $[LiO_4]$ tetrahedral units. As seen in Fig. 1, the $[MnO_4]$ and $[SiO_4]$ tetrahedral structures are in the same direction parallel to the c axis and form an inter-action arrangement in the ab plane. All tetrahedra are corner-sharing at the red oxygen atoms, and the Mn and Si ions are located at the centers of the oxygen tetrahedra. The Li ions are located between the layers of $[MnO_4]$ and $[SiO_4]$. The optimized crystal parameters of Li_2MnSiO_4 are listed in Table S1 in the ESI.† Our results are in excellent agreement with experiments and other theoretical work.[40,42,43] The good reproduction of the experimental structure provides a good starting point for our calculations.

The Li_2MnSiO_4 supercell was first optimized with zero strain applied. Subsequently, plane biaxial compressive and tensile strains were applied in the ab, ac and bc planes. By providing a strain value, the atomic position is able to be optimized satisfactorily. Using this procedure, for example, when strain is applied in the ab plane, the lattice parameter c becomes the only lattice parameter of the crystal structure for scaling behavior. Fig. 2 shows the total energy of the Li_2MnSiO_4 supercell as a function of the lattice parameter c for both compressive and tensile strain in the ab plane. The optimized total energy is obtained by employing parabolic curves. Here we use twice optimization (with two different accuracy values: 1% and 0.1%) for energy minimization to obtain the accurate lattice parameters. We can easily get the result that the introduction of positive tensile strain is more favorable than compressive strain from the total energy. When no strain is applied, optimized c
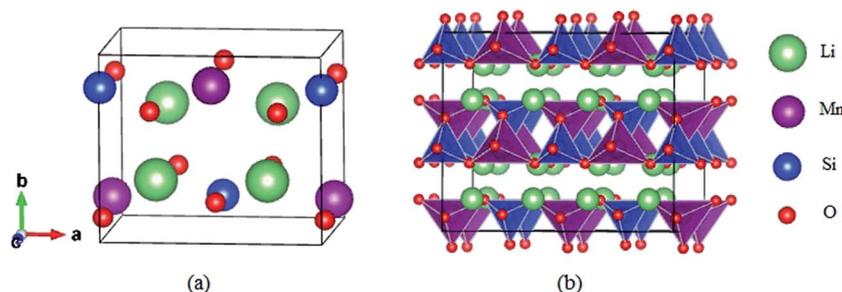
Fig. 1 Schematic crystal of Li_2MnSiO_4 with the $pmn21$ space group: (a) the unit cell, (b) polyhedral view of the $2 \times 2 \times 2$ supercell. Li ions are shown in green, Mn tetrahedra in purple and Si tetrahedra in blue; red spheres represent oxygen atoms.
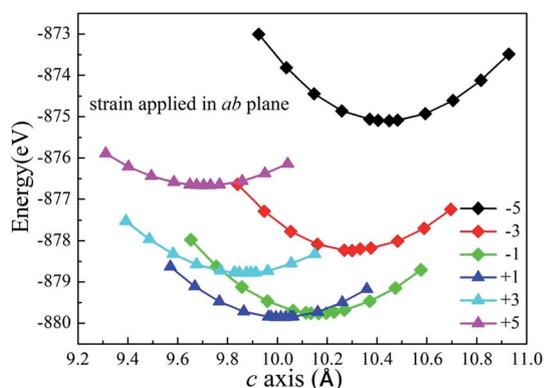

Fig. 2 Total energy for the supercell ($2 \times 2 \times 2$) of Li_2MnSiO_4 as a function of the lattice parameter c for different strain applied in the ab plane.

equals 10.065 Å, and this value is between +1% and −1% strain. With strain applied in the ac and bc planes (see Fig. S1, ESI†), we can get the same results. The strained structures of minimized energy were used as the initial configurations for ion migration and defect calculations.

In general, as a positive strain is applied in the biaxial plane, a decrease in the third parameter is observed whereas the

Fig. 3 The calculated volumes for the Li_2MnSiO_4 (corresponding to unit cell) structure under various strains applied in the ab, ac and bc planes.

volume slightly increases. When the strain is applied negatively, the third parameter increases and the volume decreases slightly.[36] Fig. 3 shows the calculated volumes with compressive and tensile strain applied. Comparing Fig. 2 and S1 (ESI†), we notice an excellent agreement of the lattice parameters and volumes with our computational results. The computed structural parameters and volumes of Li_2MnSiO_4 under six strains are summarized in Fig. S2, ESI.† All of this supports the rationality of our models and the stability of the structure under the strain applied.

3.2 Lithium ion migration in the Li_2MnSiO_4 structure

To investigate the influence of lattice strain on the Li ion diffusion behavior, first we studied the migration properties in the unstrained Li_2MnSiO_4 structure. The CI-NEB method, combined with a DFT+U approach, was used to calculate the saddle points. The lithium diffusion process uses a vacancy mechanism in the $2a \times 2b \times 2c$ supercell, which contains 31 lithium ions and one lithium vacancy. The essence of diffusion is the position exchange of a lithium vacancy and the neighboring lithium ions. For the Li_2MnSiO_4 structure, three possible migration pathways are identified: (a) pathway A – along the [100] direction, (b) pathway B – zigzag trajectory in the bc (011) crystal plane, and (c) pathway C – also in the bc plane and across the $[MnSiO_4]$ layer.

In the [100] direction, the migration steps are schematically shown in Fig. 4(a). There are two kinds of pathways according to the different surrounding environments, which are labeled from site 1 to site 2 and site 2 to site 3. The calculated activation energy for pathway A is given in Fig. 4(b). Actually, there are different twice hopping situations for different activation energies. When lithium jumps from site 1 to site 2, the activation barrier is about 0.77 eV, the jumping distance is 3.70 Å, and the neighbor of the migrating ion is a $[SiO_4]$ tetrahedron. For another removal of a Li ion from site 2 to site 3, the neighbor is a $[MnO_4]$ tetrahedron, the activation barrier is about 0.88 eV and the jumping distance is 3.60 Å. From the above results, pathway A characterizes a linear channel in the Li layer. The activation barrier energy is 0.88 eV when a lithium ion migrates by pathway A.

For the bc plane, Li ion migration along pathway B is characterized by a zigzag trajectory between the Mn–Si–O layers. The
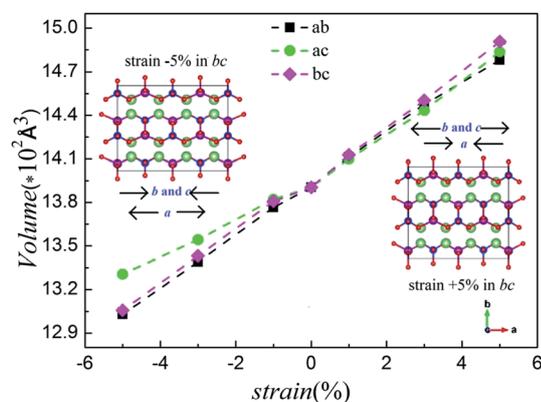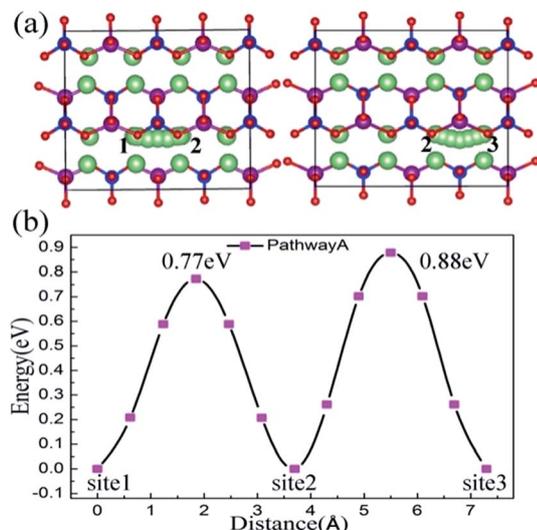
Fig. 4 Activation barriers calculated by a CI-NEB method for two available pathways. The positions of these paths in Li_2MnSiO_4 are represented by ball-stick models and five hops are included. Pathway A is parallel to the a axis and includes twice hopping. The Li ion migration steps are shown in (a), and the activation barriers are shown in (b).
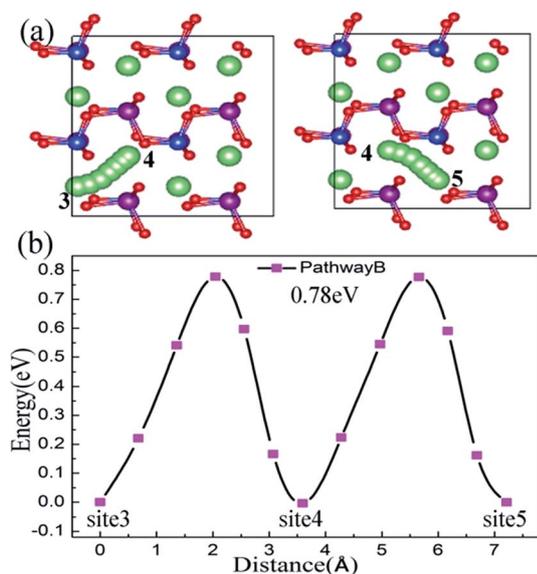

Fig. 5 Pathway B is in the bc plane, not across the $[MnSiO_4]$ layer. The Li ion migration steps are shown in (a) and activation barriers are shown in (b).

migration steps and activation barriers are schematically shown in Fig. 5(a) and (b), respectively. Pathway B also consists of twice hopping, i.e. jumping from site 3 to site 4 and then from site 4 to site 5. From the migration structure (Fig. 5(a)), the twice hopping exhibits the same migration performance. The calculated activation barrier is about 0.78 eV and the jumping distance is 3.62 Å. For pathway C, the Li ion migrates across the $[MnSiO_4]$ layer, which induces a large electrostatic repulsive interaction between Li^+ and the $[MnSiO_4]$ layer.[44] This migration

leads to a large activation barrier of 1.90 eV and the jumping distance is 4.95 Å (Fig. S3, ESI†), which are both substantially larger than the values for pathway A and pathway B. Therefore, it can be regarded as impossible that the Li ion migration follows pathway C.

In the Li_2MnSiO_4 structure, all the Li ions occupy the same Wyckoff (4b) positions. So in each migration process, jumping into or out of different Li sites, the total energy remains the same. This can be seen clearly in the activation energy curves (Fig. 4(b), 5(b) and S3, ESI†); i.e. in pathway A, the energy of the system is almost the same whether the Li vacancy is at site 1, site 2 or site 3, likewise in pathway B and pathway C. From the lithium migration result, we can infer that the Li_2MnSiO_4 compound has a two dimensional pathway for Li ion migration. This is in good agreement with other theoretical work.[11,44] Moreover, the other orthosilicate materials, Li_2FeSiO_4 and Li_2-$CoSiO_4$, also have a 2D migration of lithium ions.[45,46]

3.3 Strain effects on Li ion migration

To illustrate the relationship between lattice strain and the Li ion migration barrier energy, the activation barrier of Li_2-$MnSiO_4$ under different strains was calculated for two pathways. The lithium migrations were subjected to biaxial compressive and tensile strains between −5% and +5% in the ab, ac and bc planes. According to the migration of lithium ions in the unstrained Li_2MnSiO_4 material, here twice hopping mechanisms were calculated for pathway A and once hopping mechanisms were calculated for pathway B. The migration energy curves are shown in Fig. 6(a) and (b), (c) and (d), and (e) and (f), representing the energy when strain is applied in ab, ac and bc planes, respectively. For pathway A, the twice migration exhibits different energy barriers. We use the higher one as the lithium ion diffusion energy. Moreover, due to the crystal anisotropy, the mechanism of lithium migration shows different properties when biaxial strain is applied on different planes for Li_2MnSiO_4.

Fig. 7 shows the migration barrier along the two channels as a function of applied strain. The activation barrier increases slightly with the strain applied in the ab and ac planes for Li diffusion in pathway A ([100] direction, Fig. 7(a)). Interestingly, the activation barrier shows an obvious decrease in the bc plane. As the strain changes from −5% to 5%, the activation barrier drops from about 1.36 eV to 0.54 eV. The energy value decreases gradually with the increase of strain from negative ($\varepsilon < 0$) to positive ($\varepsilon > 0$), and by almost forty percent for the unstrained system when +5% tensile strain is applied. That is to say, the Li ion diffusion coefficient becomes larger/smaller when the a axis lattice is elongated/compressed. The mechanism of the change in lithium migration under strain is very complicated.[47] In general, the Li ion migration barrier is determined by the potential energy surface along the migration pathway, which is related to both the migration space and structural modifications.[18,19,48] From the energy minimized structures, we can obtain the result that lattice parameter a gradually decreases when strain is applied in the bc plane. Therefore, the Li–Li hopping distance for migration along the [100] direction decreases, while it increases for the other planes (Fig. S2, ESI†).
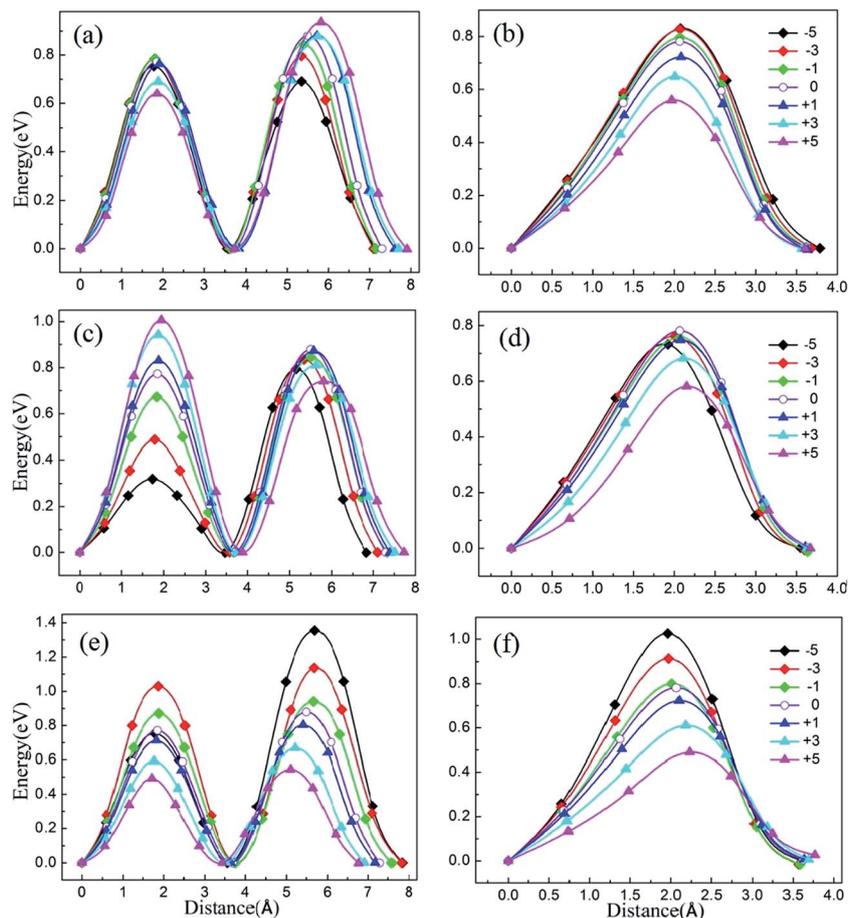
Fig. 6 The migration barriers for lithium ions under different lattice strain between −5% and +5%. According to different atomic arrangements, twice hopping mechanisms were calculated for pathway A and once hopping mechanisms were calculated for pathway B. (a) and (b), (c) and (d), and (e) and (f) represent the strain effect in the *ab*, *ac*, and *bc* planes, respectively. The left images represent pathway A; the right images represent pathway B.
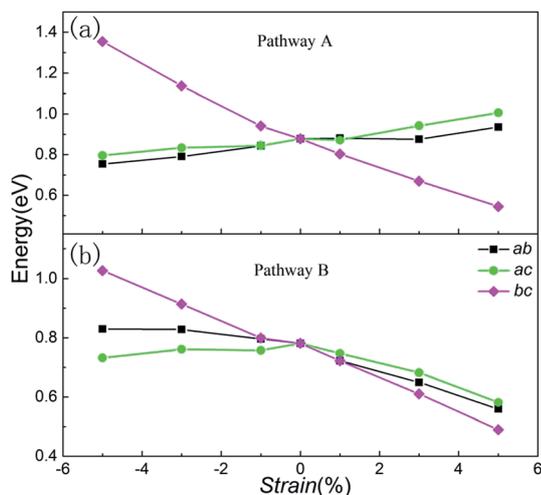

Fig. 7 Change in the lithium ion activation barriers as a function of strain for (a) pathway A and (b) pathway B.

Additionally, the available polyhedron volumes at the saddle points also influence the activation barrier. Shorter Li–Li hopping distances and larger polyhedron volumes can decrease the Li ion activation energy. This rule is also useful in olivine systems; Tealdi *et al.*[19] reported that $LiFePO_4$ and $NaFePO_4$ both have a one dimensional pathway for alkali-ion migration (along with the [010] direction). When strain is applied in $LiFePO_4$ and $NaFePO_4$, the migration energy decreases along with strain for the *ac* plane, while it increases slightly along with strain for the *ab* and *bc* planes.

Then, we start to consider Li ion migration in the *bc* plane for pathway B. We plot the activation barrier as a function of applied strain in Fig. 7(b). The activation barrier is different to that for pathway A. When strain is applied in the *ab* and *bc* planes, the lithium ion activation energy barriers decrease as a function of strain. In other words, the barriers are increased with compressive strain and reduced with tensile strain, compared to the unstrained condition. For the *ac* plane, the activation barrier has a slight change when compressive strain is applied. When tensile strain is applied it shows an obvious decrease. From our calculations, the strain-induced change of

the activation barrier in the *bc* plane is more sensitive than that imposed in the *ab* and *ac* planes. During migration of lithium ions with a zigzag trajectory in the *bc* plane (pathway B), the tensile strain applied in the *bc* plane enlarged the lattice parameters *b* and *c*. Even though this increased the Li–Li hopping distances, the available polyhedron volumes at the saddle points were increased. Finally, under both different effects for Li migration, the barrier energy decreased. As the strain changes from −5% to 5%, the activation barrier drops from 1.03 eV to 0.50 eV. For the strain applied in the *ab* and *ac* planes, the change of the activation barrier for Li migration is less sensitive than the strain in the *bc* plane.

Therefore, the above results show that lithium ion migration can be enhanced substantially for both diffusion pathways through applying tensile strain in the *bc* plane. This suggests that applying strain in the *bc* plane is an effective method for increasing the ionic conductivity, which improves the rate performance of Li_2MnSiO_4 as a cathode material. This provides a good direction for future investigations into controlling the lattice parameters. In fact, this is a great challenge for the experimental technology associated with lattice mismatch, defect effects, the Jahn–Teller effect and so on. In order to find a more accurate explanation for the correlation between Li ion migration and lattice strain, further studies are necessary.

3.4 Strain effects on defects

The inherent defect of the silicate cathode materials Li_2MSiO_4 (M = Mn, Fe, Co, Ni), which involves the exchange of Li for an M atom, can be detrimental to the ion intercalation properties:

$$Li_{Li}^\times + Mn_{Mn}^\times \rightarrow Li_{Mn}^\cdot + Mn_{Li}' \qquad (2)$$

It was reported that anti-site disorder occurred when Li_2MnSiO_4 was first experimentally synthesized,[40] with partial occupancies of Li and Mn at the 4*b* and 2*a* sites. The rearrangement of atoms in site-exchange materials influences the overall electrochemical performance.[49]

In order to determine whether the biaxial strain affects the intrinsic site-exchange defect, models with one pair of Li/Mn site-exchange (SE structure) based on the strained structures were built, and then the total energies of the defect structures were calculated. Comparing these energies with the energy of the undefective structure, we get the formation energy of one pair of Li/Mn site-exchange. Fig. 8 shows the total energy of two types of structure and the formation energy as a function of the biaxial strain in the *bc* plane for Li_2MnSiO_4. The formation of undefective Li_2MnSiO_4 is more favorable than that of the SE structure, no matter how much strain (−5% to +5%) is applied in the material. The result agrees well with other theoretical work when no strain is applied in Li_2MnSiO_4.[11] This suggests that the SE defective structure cannot be produced spontaneously in theory. Besides, from the two curves of the total energy, both the Li_2MnSiO_4 and SE structures have the highest stability without strain.

In particular, as the imposed strain increases from compressive to tensile strain, the Li/Mn site-exchange
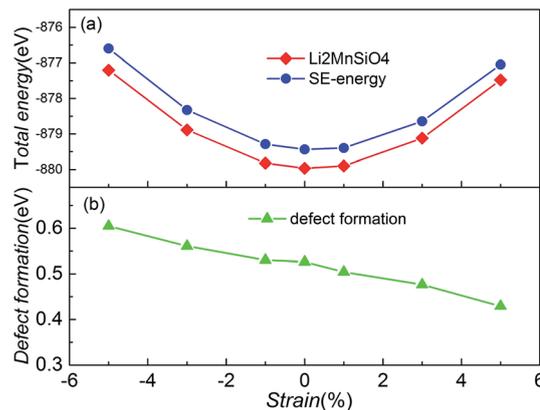

Fig. 8 (a) The total energy for the Li_2MnSiO_4 and SE structures as a function of the applied biaxial/compressive strain in the *bc* plane. (b) Formation energy of one pair of Li/Mn site-exchange, based on eqn (2).

formation energy slightly decreases. From Fig. 8(b), the formation of this defect ranges from 0.60 eV to 0.43 eV when the strain is applied from compressive −5% to tensile +5%. These values indicate that the defect is more pronounced for tensile strain. Changes in defect formation energy can be interpreted from structural modifications. Notice that the volume of the system increases gradually when the strain value increases. The increase of structural space makes the Li ion migration barrier decrease, and exchange of the defect Li and Mn sites is easier. In the $LiFePO_4$ olivine system, the exchange of a Li ion with a neighboring Fe atom is involved, but the strain effects on defect formation are different from those in Li_2MnSiO_4.[19] This suggests that the strain in $LiFePO_4$ is not a crucial parameter to modulate the Li/Fe anti-site defect population, and the anti-site formation energy does not change dramatically when the applied strain is changed from compressive −3% to tensile +3%.

Therefore, from this section the key conclusion is that the defect of Li/Mn site-exchange cannot be produced spontaneously when strain is applied in the *bc* plane for Li_2MnSiO_4. Unfortunately, the calculation of one pair Li/Mn site-exchange formation energy found that the defect is more pronounced for tensile strain. Although the strain is applied in the *bc* plane, the ionic conductivity can be greatly improved. In summary, when trying to improve the performance of Li_2MnSiO_4 by using lattice strain, both types of strain should be taken into account and an appropriate value of strain chosen.

4. Conclusions

Changing lattice strain is considered to be a promising method to modulate the structural properties of materials. In this work, we use first principles and a CI-NEB method to investigate the ionic diffusion properties of Li_2MnSiO_4 when strain is applied in the *ab*, *ac* and *bc* planes. The result from the total energy shows that the introduction of tensile strain is more favorable than that of compressive strain. More importantly, the strain applied in the *bc* plane has a remarkable effect on Li migration, and the

activation energy increases/decreases upon application of compressive/tensile strain for both pathways. For the Li_2MnSiO_4 material, the migration barriers are about 0.88 eV and 0.78 eV. These are reduced to 0.54 eV and 0.49 eV when the tensile strain is +5%. Besides, the Li/Mn anti-site defect of Li_2MnSiO_4 is also calculated, and the structure without defects has more stability than the SE system. But the formation energy of the defect decreases slightly when strain is applied. This is a slightly unfavorable modification to improve the rate performance of the material. These results suggest that an appropriate strain applied in the bc plane could improve the Li ion conductivity.

Acknowledgements

References

1 Y. K. Sun, Z. Chen, H. J. Noh, et al. Nanostructured high-energy cathode materials for advanced lithium batteries, Nat. Mater., 2012, **11**(11), 942–947.

2 D. Larcher and J. M. Tarascon, Towards greener and more sustainable batteries for electrical energy storage, Nat. Chem., 2015, **7**(1), 19–29.

3 M. D. Bhatt and C. O'Dwyer, Recent progress in theoretical and computational investigations of Li-ion battery materials and electrolytes, Phys. Chem. Chem. Phys., 2015, **17**(7), 4799–4844.

4 H. Yu, Y. G. So, A. Kuwabara, et al. Crystalline grain interior configuration affects lithium migration kinetics in Li-rich layered oxide, Nano Lett., 2016, **16**(5), 2907–2915.

5 R. J. Gummow and Y. He, Recent progress in the development of Li_2MnSiO_4 cathode materials, J. Power Sources, 2014, **253**, 315–331.

6 A. Nytén, A. Abouimrane, M. Armand, et al. Electrochemical performance of Li_2FeSiO_4 as a new Li-battery cathode material, Electrochem. Commun., 2005, **7**(2), 156–160.

7 M. E. Arroyo-de Dompablo, M. Armand, J. M. Tarascon, et al. On-demand design of polyoxianionic cathode materials based on electronegativity correlations: an exploration of the Li_2MSiO_4 system (M = Fe, Mn, Co, Ni), Electrochem. Commun., 2006, **8**(8), 1292–1298.

8 C. Lyness, B. Delobel, A. R. Armstrong, et al. The lithium intercalation compound Li_2CoSiO_4 and its behaviour as a positive electrode for lithium batteries, Chem. Commun., 2007, **46**, 4890–4892.

9 S. Q. Wu, Z. Z. Zhu, Y. Yang, et al. Structural stabilities, electronic structures and lithium deintercalation in Li_xMSiO_4 (M = Mn, Fe, Co, Ni): A GGA and GGA+U study, Comput. Mater. Sci., 2009, **44**(4), 1243–1251.

10 D. Rangappa, K. D. Murukanahally, T. Tomai, et al. Ultrathin nanosheets of Li_2MSiO_4 (M = Fe, Mn) as high-capacity Li-ion battery electrode, Nano Lett., 2012, **12**(3), 1146–1151.

11 C. A. J. Fisher, N. Kuganathan and M. S. Islam, Defect chemistry and lithium-ion migration in polymorphs of the cathode material Li_2MnSiO_4, J. Mater. Chem. A, 2013, **1**(13), 4207–4214.

12 V. Aravindan, K. Karthikeyan, K. S. Kang, et al. Influence of carbon towards improved lithium storage properties of Li_2MnSiO_4 cathodes, J. Mater. Chem., 2011, **21**(8), 2470–2475.

13 M. Zhang, S. Zhao, Q. Chen, et al. $Li_{2+x}MnSi_{1-x}Al_xO_4$/C nanoparticles for high capacity lithium-ion battery cathode applications, RSC Adv., 2014, **4**(58), 30876–30880.

14 N. Kuganathan and M. S. Islam, Li_2MnSiO_4 lithium battery material: atomic-scale study of defects, lithium mobility, and trivalent dopants, Chem. Mater., 2009, **21**(21), 5196–5202.

15 S. Zhang, Z. Lin, L. Ji, et al. Cr-doped Li_2MnSiO_4/carbon composite nanofibers as high-energy cathodes for Li-ion batteries, J. Mater. Chem., 2012, **22**(29), 14661–14666.

16 Z. L. Gong, Y. X. Li and Y. Yang, Synthesis and Characterization of $Li_2Mn_xFe_{1-x}SiO_4$ as a Cathode Material for Lithium-Ion Batteries, Electrochem. Solid-State Lett., 2006, **9**(12), A542–A544.

17 C. Deng, S. Zhang, Y. X. Wu, et al. Partial substitution of Mn/Si with V, Cr or Al in Li_2MnSiO_4 nanoparticle: dependence of the physical and electrochemical properties on the substitution strategy, J. Electroanal. Chem., 2014, **719**, 150–157.

18 F. Ning, S. Li, B. Xu, et al. Strain tuned Li diffusion in $LiCoO_2$ material for Li ion batteries: a first principles study, Solid State Ionics, 2014, **263**, 46–48.

19 C. Tealdi, J. Heath and M. S. Islam, Feeling the strain: enhancing ionic transport in olivine phosphate cathodes for Li- and Na-ion batteries through strain effects, J. Mater. Chem. A, 2016, **4**(18), 6998–7004.

20 A. M. Smith, A. M. Mohs and S. Nie, Tuning the optical and electronic properties of colloidal nanocrystals by lattice strain, Nat. Nanotechnol., 2009, **4**(1), 56–63.

21 C. W. Hicks, D. O. Brodsky, E. A. Yelland, et al. Strong increase of Tc of Sr_2RuO_4 under both tensile and compressive strain, Science, 2014, **344**(6181), 283–285.

22 X. Li, K. Maute, M. L. Dunn, et al. Strain effects on the thermal conductivity of nanostructures, Phys. Rev. B: Condens. Matter Mater. Phys., 2010, **81**(24), 245318.

23 K. Wen, W. Lv and W. He, Interfacial lattice-strain effects on improving the overall performance of micro-solid oxide fuel cells, J. Mater. Chem. A, 2015, **3**(40), 20031–20050.

24 J. Lee, S. J. Pennycook and S. T. Pantelides, Simultaneous enhancement of electronic and Li^+ ion conductivity in $LiFePO_4$, Appl. Phys. Lett., 2012, **101**(3), 033901.

25 R. A. De Souza, A. Ramadan and S. Hörner, Modifying the barriers for oxygen-vacancy migration in fluorite-structured CeO_2 electrolytes through strain: a computer simulation study, Energy Environ. Sci., 2012, **5**(1), 5445–5453.

26 G. Kresse and J. Furthmüller, Efficient iterative schemes for ab initio total-energy calculations using a plane-wave basis set, Phys. Rev. B: Condens. Matter Mater. Phys., 1996, **54**(16), 11169.

27 G. Kresse and J. Furthmüller, Efficiency of ab initio total energy calculations for metals and semiconductors using a plane-wave basis set, Comput. Mater. Sci., 1996, **6**(1), 15–50.

28 P. E. Blöchl, Projector augmented-wave method, *Phys. Rev. B: Condens. Matter Mater. Phys.*, 1994, **50**(24), 17953.

29 J. P. Perdew, K. Burke and M. Ernzerhof, Generalized gradient approximation made simple, *Phys. Rev. Lett.*, 1996, **77**(18), 3865.

30 V. I. Anisimov, J. Zaanen and O. K. Andersen, Band theory and Mott insulators: Hubbard U instead of Stoner I, *Phys. Rev. B: Condens. Matter Mater. Phys.*, 1991, **44**(3), 943.

31 H. J. Monkhorst and J. D. Pack, Special points for Brillouin-zone integrations, *Phys. Rev. B: Solid State*, 1976, **13**(12), 5188.

32 M. E. Arroyo-de Dompablo, M. Armand, J. M. Tarascon, *et al.* On-demand design of polyoxianionic cathode materials based on electronegativity correlations: an exploration of the Li_2MSiO_4 system (M = Fe, Mn, Co, Ni), *Electrochem. Commun.*, 2006, **8**(8), 1292–1298.

33 G. Zhong, Y. Li, P. Yan, *et al.* Structural, Electronic, and Electrochemical Properties of Cathode Materials Li_2MSiO_4 (M = Mn, Fe, and Co): Density Functional Calculations, *J. Phys. Chem. C*, 2010, **114**(8), 3693–3700.

34 K. Wen, K. H. L. Zhang, W. Wang, *et al.* Physical justification for ionic conductivity enhancement at strained coherent interfaces, *J. Power Sources*, 2015, **285**, 37–42.

35 P. Strasser, S. Koh, T. Anniyev, *et al.* Lattice-strain control of the activity in dealloyed core–shell fuel cell catalysts, *Nat. Chem.*, 2010, **2**(6), 454–460.

36 C. Ferrara, C. Eames, M. S. Islam, *et al.* Lattice strain effects on doping, hydration and proton transport in scheelite-type electrolytes for solid oxide fuel cells, *Phys. Chem. Chem. Phys.*, 2016, **18**(42), 29330–29336.

37 C. Tealdi and P. Mustarelli, Improving oxygen transport in perovskite-type $LaGaO_3$ solid electrolyte through strain, *J. Phys. Chem. C*, 2014, **118**(51), 29574–29582.

38 G. Henkelman, B. P. Uberuaga and H. Jónsson, A climbing image nudged elastic band method for finding saddle points and minimum energy paths, *J. Chem. Phys.*, 2000, **113**(22), 9901–9904.

39 G. Henkelman and H. Jónsson, Improved tangent estimate in the nudged elastic band method for finding minimum energy paths and saddle points, *J. Chem. Phys.*, 2000, **113**(22), 9978–9985.

40 R. Dominko, M. Bele and M. Gaberšček, *etal.* Structure and electrochemical performance of Li_2MnSiO_4 and Li_2FeSiO_4 as potential Li-battery cathode materials, *Electrochem. Commun.*, 2006, **8**(2), 217–222.

41 A. Nytén, A. Abouimrane, M. Armand, *et al.* Electrochemical performance of Li_2FeSiO_4 as a new Li-battery cathode material, *Electrochem. Commun.*, 2005, **7**(2), 156–160.

42 H. Lee, S. D. Park, J. Moon, *et al.* Origin of poor cyclability in Li_2MnSiO_4 from first-principles calculations: layer exfoliation and unstable cycled structure, *Chem. Mater.*, 2014, **26**(13), 3896–3899.

43 M. E. Arroyo-deDompablo, R. Dominko, J. M. Gallardo-Amores, *et al.* On the energetic stability and electrochemistry of Li_2MnSiO_4 polymorphs, *Chem. Mater.*, 2008, **20**(17), 5574–5584.

44 N. Kuganathan and M. S. Islam, Li_2MnSiO_4 lithium battery material: atomic-scale study of defects, lithium mobility, and trivalent dopants, *Chem. Mater.*, 2009, **21**(21), 5196–5202.

45 A. Liivat and J. O. Thomas, Li-ion migration in Li_2FeSiO_4-related cathode materials: a DFT study, *Solid State Ionics*, 2011, **192**(1), 58–64.

46 P. Zhang, X. D. Li, S. Yu, *et al.* Effects of Na Substitution on Li Ion Migration in Li_2CoSiO_4 Cathode Material, *J. Electrochem. Soc.*, 2013, **160**(4), A658–A661.

47 H. J. Yan, Z. Q. Wang, B. O. Xu, *et al.* Strain induced enhanced migration of polaron and lithium ion in λ-MnO_2, *Funct. Mater. Lett.*, 2012, **5**(04), 1250037.

48 Y. Shin, H. Ding and K. A. Persson, Revealing the Intrinsic Li Mobility in the Li_2MnO_3 Lithium-Excess Material, *Chem. Mater.*, 2016, **28**(7), 2081–2088.

49 L. Li, L. Zhu, L. H. Xu, *et al.* Site-exchange of Li and M ions in silicate cathode materials Li_2MSiO_4 (M = Mn, Fe, Co and Ni): DFT calculations, *J. Mater. Chem. A*, 2014, **2**(12), 4251–4255.